Pyrene Excimer Fluorescence: A Spatially Sensitive Probe To Monitor Lipid-Induced Helical Rearrangement of Apolipophorin III[†]

Daisy Sahoo,[‡] Vasanthy Narayanaswami,[‡] Cyril M. Kay,[§] and Robert O. Ryan*[,‡]

Lipid and Lipoprotein Research Group, Protein Engineering Network Centres of Excellence, Department of Biochemistry, University of Alberta, Edmonton, Alberta T6G 2S2, Canada

Received November 10, 1999; Revised Manuscript Received March 27, 2000

ABSTRACT: *Manduca sexta* apolipophorin III (apoLp-III), an 18-kDa, monomeric, insect hemolymph apolipoprotein, is comprised of five amphipathic α-helices arranged as a globular bundle in the lipid-free state. Upon lipid binding, it is postulated that the bundle opens, exposing a continuous hydrophobic surface which becomes available for lipid interaction. To investigate lipid binding-induced helical rearrangements, we exploited the unique fluorescence characteristics of *N*-(1-pyrene)maleimide. Pyrene is a spatially sensitive extrinsic fluorescent probe, which forms excited-state dimers (excimers) upon close encounter with another pyrene molecule. Cysteine residues were introduced into apoLp-III (which otherwise lacks cysteine) at Asn 40 (helix 2) and/or Leu 90 (helix 3), creating two single-cysteine mutants (N40C-apoLp-III and L90C-apoLp-III) and N40C/L90C-apoLp-III, a double-cysteine mutant, which were labeled with pyrene maleimide. Pyrene-labeled N40C/L90C-apoLp-III, but not the pyrene-labeled single-cysteine mutants, exhibited strong excimer fluorescence in the lipid-free, monomeric state. Guanidine hydrochloride titration and temperature studies revealed a loss in excimer fluorescence, accompanied by a loss in the molar ellipticity of the protein. When apoLp-III interacts with phospholipid vesicles to form disklike complexes, a significant loss in excimer fluorescence was noted, indicating that the helices bearing the pyrene moieties diverge from each other. Pyrene excimer fluorescence was further employed to examine the relative orientation of lipid-bound apoLp-III molecules. Pyrene-labeled N40C- or L90C-apoLp-III displayed no excimer fluorescence in the disk complexes, while complexes prepared with an equal mixture of both single-labeled mutants did emit excimer fluorescence, indicating apoLp-III adopts a preferred nonrandom orientation around the perimeter of the bilayer disk. These studies establish pyrene excimer fluorescence as a useful spectroscopic tool to address intra- and intermolecular interactions of exchangeable apolipoproteins upon binding to lipid.

Plasma lipoprotein interconversions and metabolism are modulated by the presence of exchangeable apolipoproteins (*1*). An inherent structural adaptability of these predominantly α-helical proteins allows them to exist in both lipid-free and lipid-bound states. Apolipophorin III (apoLp-III)[1] from the Sphinx moth, *Manduca sexta*, is a well-characterized exchangeable apolipoprotein with physicochemical and functional properties characteristic of this protein class (*2*). Heteronuclear multidimensional NMR studies have provided key structural information for *M. sexta* apoLp-III in the absence of lipid (*3*). ApoLp-III adopts a globular conformation, consisting of a bundle of five amphipathic α-helices organized in an up-and-down antiparallel manner. In this configuration, the hydrophobic faces of the amphipathic helices orient toward the interior of the bundle, while polar and charged residues orient toward the aqueous environment. It has been postulated that, upon lipid interaction, the bundle opens about putative hinge loops such that helices 1, 2, and 5 move away from helices 3 and 4 (*4*−*6*). A fundamental aspect of this proposed conformational change is substitution of helix−helix interactions, which stabilize the bundle conformation, by helix−lipid interactions, which stabilize the lipid-bound conformation. Importantly, this conformational change is readily reversible and, apparently, occurs without a significant alteration in the length or number of helical segments known to exist in the globular helix bundle (*3*, *7*). In the present study, we explore the unique fluorescence properties of *N*-(1-pyrene)maleimide, an intensely fluorescent extrinsic cysteine-reactive probe, which displays unique spectral characteristics such as the ability to form excited-state dimers (excimers) when spatially proximal to another pyrene molecule. We exploit pyrene excimer fluorescence to address the following issues: lipid binding-induced helix repositioning in apoLp-III and the relative orientation of lipid-bound apoLp-III in model phospholipid disk complexes.

EXPERIMENTAL PROCEDURES

Materials. *N*-(1-Pyrene)maleimide and tris(2-cyanoethyl)-phosphine were obtained from Molecular Probes, Inc.

[†] This work was supported by a grant from the Medical Research Council of Canada.

* To whom correspondence should be addressed at 328 Heritage Medical Research Centre, University of Alberta, Edmonton, Alberta, T6G 2S2 Canada. Tel: (780) 492-5153. Fax: (780) 492-3383. E-mail: Robert.Ryan@Ualberta.ca.

[‡] Lipid and Lipoprotein Research Group.

[§] Protein Engineering Network Centres of Excellence.

[1] Abbreviations: apoLp-III, apolipophorin III; GdnHCl, guanidine hydrochloride; DMPC, dimyristoylphosphatidylcholine; TFE, trifluoroethanol.

10.1021/bi992609m CCC: $19.00
Published on Web 05/12/2000

(Eugene, OR). Bis-maleimidohexane was from Pierce (Rockford, IL). Dimyristoylphosphatidylcholine (DMPC) and dimethyl sulfoxide were from Sigma (St. Louis, MO). All other chemicals and solvents were of analytical grade.

Protein Expression and Pyrene Modification. Cysteine residues were introduced into apoLp-III (which otherwise lacks cysteine) by site-directed mutagenesis, as described earlier (*5*). Asn 40 (N-terminus of helix 2) and/or Leu 90 (C-terminus of helix 3) were replaced by Cys to create three mutant apoLp-IIIs: N40C -, L90C-, and N40C/L90C-apoLp-III. Recombinant wild-type and cysteine-containing mutant apoLp-IIIs were expressed in *Escherichia coli* BL21 cells and purified as described earlier (*8*). The N40C- and L90C-apoLp-III single-cysteine mutants were labeled with *N*-(1-pyrene)maleimide according to Sahoo et al. (*9*). To label the double-cysteine mutant with pyrene, N40C/L90C-apoLp-III was first incubated with a 2-fold molar excess of dithiothreitol for 2 h at 37 °C in order to maintain the sulfhydryls in a reduced state and avail them for labeling. *N*-(1-Pyrene)-maleimide was solubilized in dimethyl sulfoxide and incubated with N40C/L90C-apoLp-III (in 100 mM sodium phosphate, pH 7.5) in the dark for 2.5 h at 37 °C at a labeling ratio of 4 mol of pyrene:1 mol of protein. Unbound pyrene and pyrene−dithiothreitol were removed by gel filtration chromatography. The proteins were analyzed by SDS−polyacrylamide gel electrophoresis and visualized under UV-light. Electrospray mass spectrometry was performed using a VG quattro electrospray mass spectrometer (Fisons Instruments, Manchester, U.K.).

Fluorescence Measurements. Fluorescence spectra were recorded on a Perkin-Elmer MPF-44B spectrofluorometer equipped with a thermostated cell maintained at 20 °C. Unless otherwise specified, 100 mM sodium phosphate, pH 7.5, was used in all fluorescence experiments. Absorbance of samples was kept below 0.02 to minimize inner filter effects, and corrections were made for light scattering. A slit width of 5 nm was used for both excitation and emission monochromators. Excitation spectra were collected by setting the emission wavelengths at 375 or 460 nm for monomer and excimer, respectively. Emission spectra were collected by setting the excitation wavelength at 345 nm. Solvent background was subtracted, and the spectra were corrected for variations in sensitivity. For all calculations, the area under the monomer emission was calculated from 370 to 410 nm, while the area under the excimer emission was calculated from 440 to 510 nm. Monomer to excimer (*m*/*e*) ratios were calculated by dividing the monomer fluorescence emission intensity at 375 nm by the excimer fluorescence emission intensity at 460 nm.

Structural Characterization. The effect of pyrene modification on the secondary structure content of apoLp-III (in 50 mM sodium phosphate, pH 7.0) was evaluated by circular dichroism (CD) spectroscopy. Spectra were collected on a Jasco J-720 spectropolarimeter at 25 °C as described earlier (*10*). For guanidine hydrochloride (GdnHCl) denaturation experiments, 50 μg/mL solutions of pyrene-labeled N40C- or N40C/L90C-apoLp-III were incubated with increasing amounts of GdnHCl (final concentrations ranging from 0 to 5 M GdnHCl) for 20 h at 4 °C prior to fluorometric analysis. Relative molar ellipticity at 222 nm (θ/θ_o) was calculated by dividing the molar ellipticity at each GdnHCl concentration (θ) by the molar ellipticity in the absence of GdnHCl (θ_o). M/M_o and E/E_o represent the area under the monomer or excimer emission at each GdnHCl concentration divided by the area under the monomer or excimer emission in the absence of GdnHCl. For trifluoroethanol (TFE) experiments, 50 μg/mL solutions of pyrene-labeled N40C- or N40C/L90C-apoLp-III were incubated with increasing amounts of TFE [final concentrations ranging from 0% to 60% TFE (v/v)] for 1 min and then subjected to fluorometric analysis. M/M_o and E/E_o represent the area under the monomer or excimer emission at each TFE concentration divided by the area under the monomer or excimer emission in the absence of TFE, respectively. For temperature experiments, a circulating water bath was used to maintain the temperature in the cuvette (ranging from 20 to 70 °C) of 50 μg/mL solutions of pyrene-labeled N40C- or N40C/L90C-apoLp-III. θ/θ_{20} was calculated by dividing θ at each temperature by θ at 20 °C. M/M_{20} and E/E_{20} were calculated by dividing the area at each temperature by the area at 20 °C.

Formation of ApoLp-III−Lipid Complexes. DMPC vesicles were transformed into discoidal complexes by addition of wild-type or pyrene-labeled mutant apoLp-III as described (*6*). Phospholipid disk complexes with bound apoLp-III were isolated and separated from unbound apoLp-III by density gradient ultracentrifugation. The final lipid:protein molar ratio was ~150:1.

Cross-Linking of N40C/L90C-ApoLp-III. Lipid-free N40C/L90C-apoLp-III and DMPC-bound N40C/L90C-apoLp-III were reduced with a 2-fold molar excess of 25 mM tris(2-cyanoethyl)phosphine (in dimethyl sulfoxide) for 2 h at 37 °C. Phosphate-buffered saline (pH 7.0) and 25 mM bis-maleimidohexane (final concentration 1.25 mM) were added, and the solutions were incubated overnight at room temperature. Samples were dried under vacuum, resuspended in nonreducing sample treatment buffer, electrophoresed on a precast 8−25% SDS gradient gel on the PhastSystem (Amersham Pharmacia Biotech), and visualized using the Phast silver staining protocol.

Analytical Procedures. The bicinchoninic acid assay (Pierce Chemcial Co., Rockford, IL) was used to determine protein concentrations, while an enzyme-based colorimetric assay (Wako Pure Chemical Industries, Ltd., Osaka, Japan) was used to measure phosphatidylcholine content.

RESULTS

Characterization of Pyrene-Labeled ApoLp-III. In the reduced state, the sulfhydryl groups in N40C/L90C-apoLp-III are accessible for labeling with pyrene maleimide in the absence of denaturants. When viewed under a UV illuminator following SDS−polyacrylamide gel electrophoresis, pyrene-labeled, but not unmodified apoLp-III, was intensely fluorescent (data not shown). The extent of pyrene incorporation into N40C-, L90C-, and N40C/L90C-apoLp-III (18 371 ± 3, 18 371 ± 2, 18 379 ± 3 Da, respectively) was evaluated by electro-spray mass spectrometry. For mutant apoLp-IIIs possessing one cysteine residue, a single major mass peak was observed with a molecular mass increment of 297 Da. In the case of the apoLp-III mutant with two cysteine residues, a single mass peak corresponding to an increment of 594 Da was observed. Labeling stoichiometry was calculated using the molar extinction of pyrene as 40×10^{-3} M^{-1} cm^{-1} (*11*). Based on mass spectrometry data, we

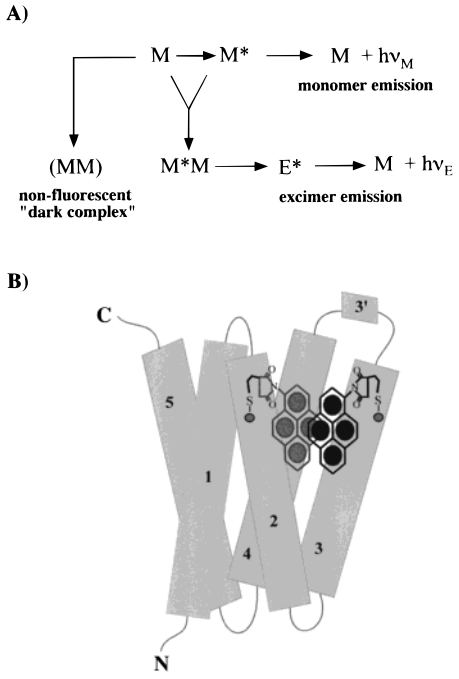

FIGURE 1: (A) Schematic representation of pyrene fluorescence properties. Excitation (345 nm) of ground-state monomers (M) gives rise to excited-state monomers (M*) with typical emission maxima at 375 and 395 nm. When M* interacts with a spatially proximal M in a precise configuration, the resulting M*M dimer results in excimer emission (E*) at 460 nm. If the dimeric configuration is not favorable for excimer emission, a nonfluorescent "dark complex" will form [modified from (*31*)]. (B) An exaggerated schematic of stacking interactions resulting in excimer fluorescence in pyrene-labeled lipid-free N40C/L90C-apoLp-III.

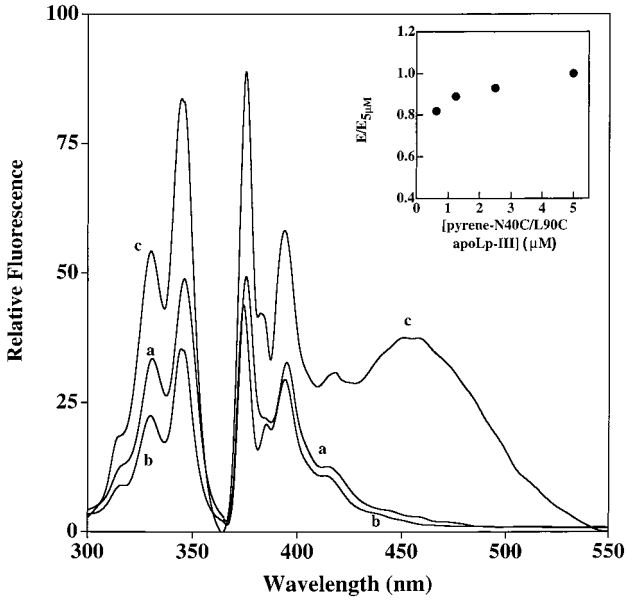

FIGURE 2: Fluorescence excitation and emission spectra of lipid-free pyrene-labeled apoLp-IIIs. Solutions (50 μg/mL) of pyrene-N40C- (curve a), pyrene-L90C- (curve b), or pyrene-N40C/L90C-apoLp-III (curve c) were excited at 345 nm, and emission was monitored between 360 and 550 nm. Excitation spectra were collected by setting the monomer emission at 375 nm. Inset: Effect of dilution on pyrene-labeled apoLp-III excimer fluorescence. $E_{5\mu M}$ represents the area under the excimer emission of a 5 μM pyrene-labeled apoLp-III solution, and E represents the area under the excimer emission at each concentration.

conclude that pyrene incorporation into the different cysteine mutants was >95%, with no evidence of unlabeled protein. Far-UV CD spectroscopy in buffer revealed that the secondary structure content of pyrene-labeled N40C/L90C-apoLp-III (67% α-helix) was similar to that of wild-type apoLp-III reported earlier (*10*). Interestingly, covalent attachment of pyrene to the double mutant increases the protein's ability to resist denaturation by GdnHCl [transition midpoint 0.35 M (*10*) for wild-type apoLp-III and 1.2 M for pyrene-labeled N40C/L90C-apoLp-III].

Pyrene Excimer Fluorescence. Pyrene maleimide, when specifically attached to free sulfhydryl groups on target proteins, exhibits unique spectral properties which are dependent upon its relative proximity to neighboring pyrene molecules. Thus, an excited-state monomer is capable of emitting typical emission bands at 375 and 395 nm (excitation 345 nm), which are attributed to monomeric pyrene moieties, as well as interacting with a suitably positioned ground-state pyrene to form excited-state dimers or "excimers" (Figure 1). Excimers occupy a lower energy excited state than an excited monomer, and give rise to a characteristic fluorescence emission upon returning to the ground state. Compared to monomer fluorescence, excimer emission is red-shifted and lacks the fine structure which arises from vibrational transitions. Thus, excimer emission results in departure from the mirror-image rule of excitation and emission spectra (*12*). Furthermore, when two pyrene moieties giving rise to excimer fluorescence reposition >10 Å from one another (e.g., due to conformational change in the labeled protein), excimer fluorescence is decreased or lost entirely. Using the structure of lipid-free apoLp-III as a guide for site-directed mutagenesis (*3*), we have placed two reactive cysteine residues into the protein at positions which are distal in terms of the linear sequence, yet proximal in terms of the three-dimensional fold of the protein. We hypothesized that covalent attachment of pyrene at these sites will result in manifestation of excimer fluorescence. Upon complexation to lipid, we predict that changes in excimer fluorescence will occur as a result of conformational opening of the helix bundle. At the same time, it is recognized that any change in monomer fluorescence could also influence excimer fluorescence. For example, if monomer fluorescence is independently quenched, the decreased population of excited monomer will result in a decreased excimer population. Thus, interpretation of changes in excimer fluorescence and assignment of such changes to increased distance between pyrene moieties must include appropriate controls.

Fluorescence Properties of Lipid-Free Pyrene-Labeled ApoLp-III. In the lipid-free α-helix bundle state, Asn 40 is located at the N-terminal end of helix 2, while Leu 90 is located at the C-terminal end of helix 3. In the up-and-down amphipathic α-helix bundle, these residues reside approximately 9 Å from one another (*3*). Fluorescence spectra were acquired for pyrene-labeled lipid-free N40C- and L90C-apoLp-III (Figure 2, curves a, b). In both cases, corresponding excitation and emission spectra are mirror images of each other at the concentrations used, with defined major emission maxima (excitation at 345 nm) at 375 and 395 nm and minor peaks at 385 and 410 nm, characteristic of pyrene monomers. In the case of N40C/L90C-apoLp-III (Figure 2, curve c), in addition to the emission maxima for monomeric pyrene, a red-shifted, significantly unstructured maximum centered around 460 nm, typical of excimer fluorescence, was

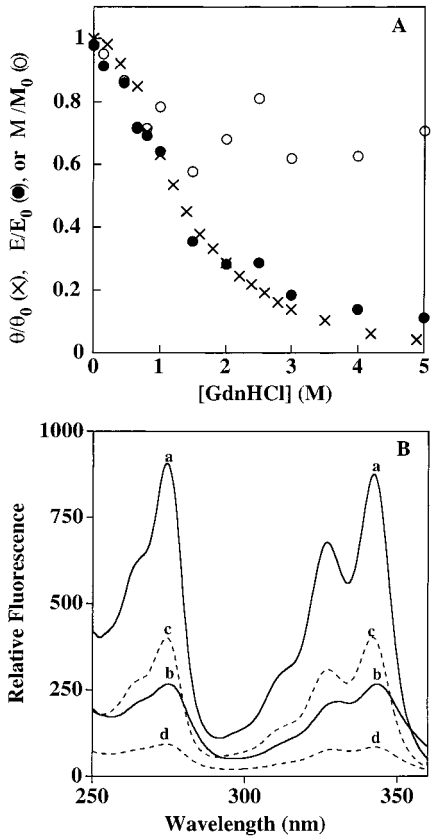

FIGURE 3: Panel A: Effect of GdnHCl on the secondary structure content and fluorescence of pyrene-N40C/L90C-apoLp-III. Aliquots of 6 M GdnHCl were added to solutions of pyrene-labeled N40C/L90C-apoLp-III (50 μg/mL). CD and fluorescence data, plotted as a function of GdnHCl concentration where molar ellipticity (θ), monomer emission (M), and excimer emission (E) are indicated by ×, ○, and ●, respectively. Values for θ/θ_o, M/M_o, and E/E_o were obtained as described under Experimental Procedures. Panel B: Excitation spectra of pyrene-labeled N40C/L90C-apoLp-III in the absence (solid lines) and presence (dashed lines) of GdnHCl. Monomer excitation spectra at 0 M GdnHCl (curve a) and 5 M GdnHCl (curve c) were collected by setting the emission wavelength at 375 nm, while excimer excitation spectra at 0 M GdnHCl (curve b) and 5 M GdnHCl (curve d) were collected by setting the emission wavelength at 460 nm.

observed. Excimer emission was noted at concentrations ranging from 0.6 to 5 μM, with little deviation in the ratio of monomer to excimer emission (Figure 2, inset). The data are consistent with the conclusion that intramolecular, rather than intermolecular, pyrene−pyrene interactions are responsible for the observed excimer fluorescence. This interpretation is supported by the lack of excimer fluorescence in apoLp-III molecules bearing a single pyrene moiety and the known existence of lipid-free apoLp-III as a monomer in buffer (*3*).

Effect of ApoLp-III Unfolding on Pyrene Excimer Fluorescence. Pyrene-labeled N40C/L90C-apoLp-III was exposed to increasing amounts of GdnHCl or heat (Figures 3 and 4, respectively). These unfolding experiments were performed to test the hypothesis that changes in apoLp-III conformation will be manifest by changes in intramolecular excimer fluorescence. In the case of GdnHCl, unfolding was judged by molar ellipticity at 222 nm and correlated with the area under the fluorescence excimer emission peak (excitation 345 nm) (Figure 3, panel A). The GdnHCl transition midpoint, monitored either by molar ellipticity or by excimer fluorescence, was 1.2 M. Although excimer fluorescence steadily decreased with increasing GdnHCl, this was not accompanied by a corresponding increase in monomer fluorescence. To assess whether the observed decrease in monomer fluorescence was due to environmental quenching, additional experiments were performed. The apparent quenching was not due to dissolved oxygen (*12*), since no differences were noted upon extensive degassing of all solutions. Likewise, the apparent quenching occurred when single pyrene-labeled N40C-apoLp-III was used (data not shown), suggesting it is unrelated to the presence of excimer fluorescence. Regardless of the cause of the decrease in monomer fluorescence as a function of GdnHCl, this phenomenon precludes a direct correlation between GdnHCl-induced unfolding of apoLp-III and loss of excimer fluorescence. To obtain information about the ground-state configuration of the pyrenes under different conditions, excitation spectra of monomer (emission 375 nm) and excimer (emission 460 nm) fluorescence were collected for pyrene-labeled N40C/L90C-apoLp-III in 0 and 5 M GdnHCl (Figure 3, panel B). In the absence of GdnHCl, there was a broadening and a small red shift of the excimer excitation spectrum (curve b) compared to that of the monomer (curve a). In addition, in the presence of 5 M GdnHCl, the excimer excitation peak (curve d) was further broadened compared not only to that of its corresponding monomer (curve c) but also to the excimer excitation spectrum at 0 M GdnHCl (curve b). These data suggest that, despite denaturation of the protein, the pyrene rings interact in the ground state, and that excimer fluorescence originates from pyrenes that are in a different environment than pyrenes that produce monomer fluorescence (*13, 14*). Thus, even at high GdnHCl, wherein there is total loss of ellipticity, pyrenes can still interact.

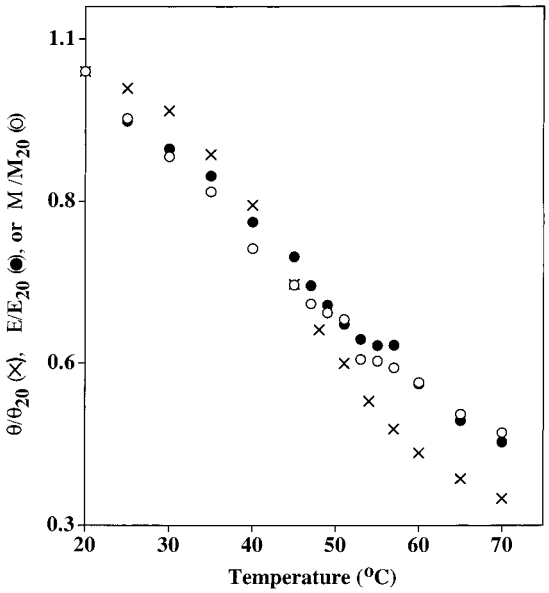

FIGURE 4: Effect of heat on pyrene excimer fluorescence. Molar ellipticity (θ) and monomer (M) and excimer (E) fluorescence of pyrene-labeled N40C/L90C-apoLp-III were followed as a function of increasing temperature. θ/θ_{20} (×), M/M_{20} (○), and E/E_{20} (●) were obtained as described under Experimental Procedures.

The same pattern is even more striking in the case of temperature-induced unfolding of pyrene-labeled N40C/L90C-apoLp-III (Figure 4). Although CD reveals that the molar ellipticity of pyrene-labeled N40C/L90C-apoLp-III is

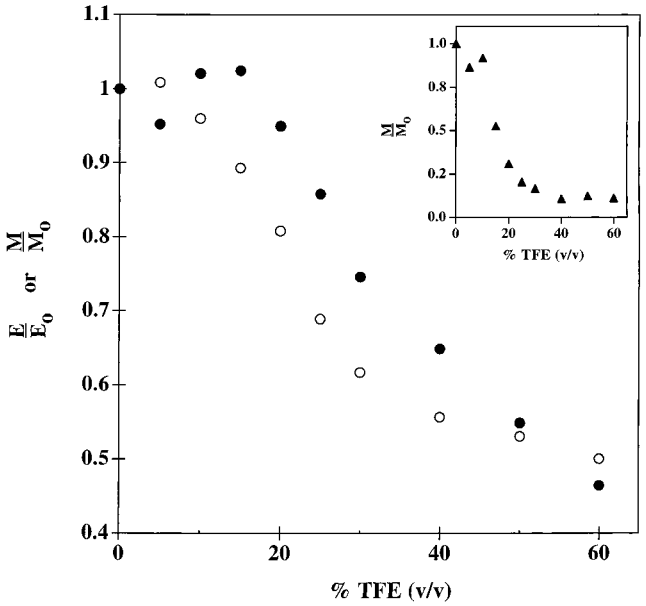

FIGURE 5: Effect of TFE on fluorescence of pyrene-labeled apoLp-III. Aliquots of 100% TFE were added to solutions of pyrene-labeled N40C/L90C-apoLp-III (50 μg/mL). Monomer (M) and excimer (E) fluorescence spectra were collected at increasing TFE concentrations. Values for M/M_o (○) and E/E_o (●) were obtained as described under Experimental Procedures. Inset: Effect of TFE on monomer fluorescence of single pyrene-labeled N40C-apoLp-III.

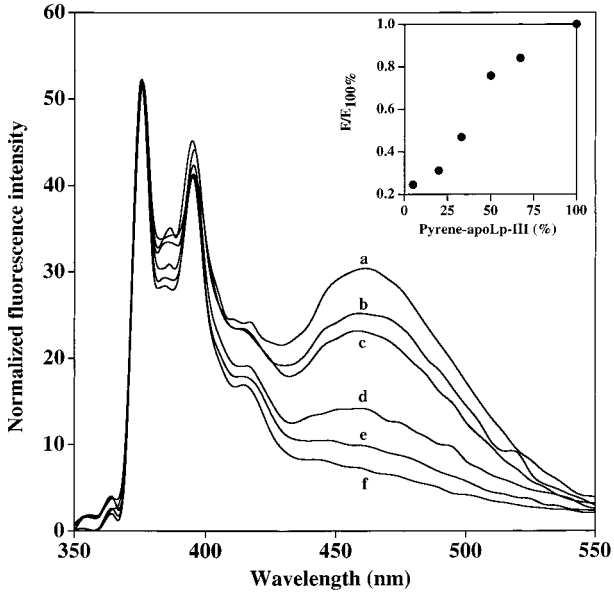

FIGURE 6: Fluorescence emission spectra of pyrene-N40C/L90C-apoLp-III bound to phospholipid bilayer disks. Pyrene fluorescence emission spectra were recorded for discoidal complexes made with only pyrene-N40C/L90C-apoLp-III (curve a; $E_{100\%}$) or a mixture of labeled N40C/L90C-apoLp-III and unlabeled wild-type apoLp-III, where the proportion of labeled apoLp-III was 67% (curve b), 50% (curve c), 33% (curve d), 20% (curve e), and 5% (curve f). The lipid:protein ratio (w/w) was maintained at 2.5:1. For the various dilutions, the monomer fluorescence was normalized on the basis of the emission peak at 375 nm. Inset: Effect of dilution on excimer fluorescence. $E_{100\%}$ represents the area under excimer emission of disks containing only pyrene-labeled apoLp-III, and E represents the area under the excimer emission of disks bearing the indicated percentage of labeled apoLp-III.

lost due to heat-induced unfolding of the protein, loss in excimer fluorescence is coincident with temperature-induced quenching of pyrene monomer fluorescence. Thus, it is not possible to attribute temperature-induced changes in excimer fluorescence directly to unfolding of apoLp-III. Excitation spectra of double pyrene-labeled apoLp-III at 20 and 70 °C revealed a similar broadening of excimer excitation spectra compared to the monomer excitation spectra, suggesting the presence of stacked pyrenes (data not shown).

Interaction of Pyrene-Labeled N40C/L90C-ApoLp-III with Trifluoroethanol. Trifluoroethanol has often been used as a helix-stabilizing cosolvent (*15*−*17*) that disrupts tertiary structural interactions in proteins while stabilizing secondary structural elements. In the case of helix bundle apolipoproteins, previous studies (*2*, *18*) suggest that TFE induces conformational opening of the helix bundle in a manner analogous to lipid interaction. Figure 5 shows the effect of TFE titration on excimer fluorescence in pyrene-labeled N40C/L90C-apoLp-III. An initial small increase in excimer fluorescence at about 10% TFE is followed by a steady decline with a maximal decrease in excimer fluorescence occurring above 60% TFE (v/v). As in the case of the temperature experiment, however, the progressive decrease in area under the excimer curve is accompanied by a corresponding decrease in monomer fluorescence, albeit with a small initial lag. It should be noted that the monomer fluorescence of single pyrene-labeled N40C-apoLp-III is also quenched by increasing concentrations of TFE (Figure 5, inset). Thus, direct correlation of loss of excimer fluorescence with presumed TFE-induced conformational opening of the helix bundle is not possible because of corresponding TFE- and/or solvent-induced quenching of monomer fluorescence.

Helical Repositioning of Pyrene-Labeled ApoLp-III on Discoidal Complexes. Amphipathic exchangeable apolipoproteins are characterized by their ability to transform phospholipid bilayer vesicles into discoidal structures (*6*). The discoidal complexes formed generally possess several apolipoprotein molecules, aligned around the perimeter of a disk-shaped phospholipid bilayer (*6*). The currently held hypothesis is that the apoLp-III helix bundle opens about hinged loops at one end of the molecule to expose the hydrophobic interior of the protein which interacts with otherwise exposed phospholipid fatty acyl chains around the perimeter of the bilayer disk. Using pyrene-labeled N40C/L90C-apoLp-III, we postulated that a loss in excimer fluorescence would occur as a result of complexation of apoLp-III with DMPC. DMPC-bound pyrene-labeled N40C/L90C-apoLp-III, however, displayed a strong excimer peak, similar to that noted for lipid-free pyrene-apoLp-III (Figure 6, curve a). Since apoLp-III/DMPC disk complexes possess up to six molecules of apoLp-III per particle (*6*), we hypothesized that intermolecular pyrene−pyrene interactions may be contributing to excimer fluorescence observed on apoLp-III/DMPC disk complexes. To discern between intramolecular and intermolecular excimer formation, dilution experiments using unlabeled wild-type protein were performed. Thus, during preparation of the disk complexes, pyrene-labeled N40C/L90C-apoLp-III was mixed with increasing amounts of wild-type apoLp-III. A gradual loss of excimer fluorescence was observed when the percentage of unlabeled protein on the disk was increased (Figure 6, curves b−f). Importantly, the loss in excimer fluorescence (Figure 6, inset) was accompanied by a steady increase in the m/e ratio, corrected for dilution (m/e ratio of 1.7 for curve b

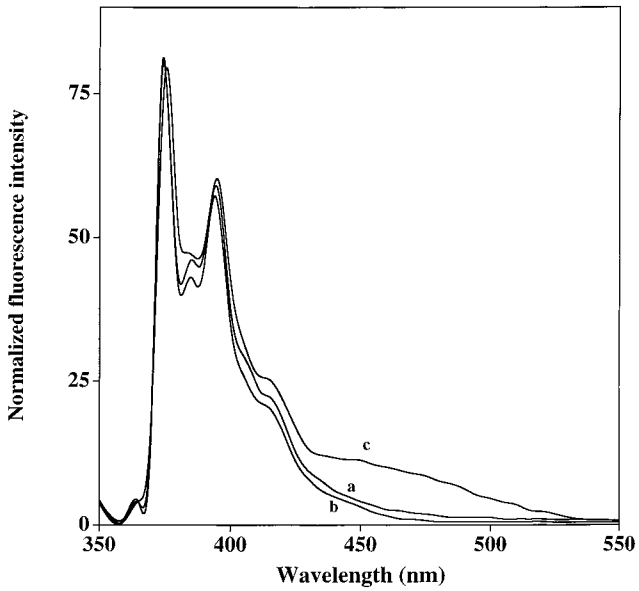

FIGURE 7: Fluorescence emission spectra of single pyrene-labeled apoLp-III/DMPC disks. Emission spectra were collected for DMPC complexes containing pyrene-N40C-apoLp-III (curve a), pyrene-L90C-apoLp-III (curve b), or equal amounts of pyrene-N40C- and pyrene-L90C-apoLp-III (curve c). The lipid:protein ratio was 2.5:1. Monomer fluorescence was normalized on the basis of the emission peak at 375 nm.

increasing to 7.2 for curve f). It is therefore rationalized that excimer fluorescence observed on disks bearing only pyrene-labeled N40C/L90C-apoLp-III arises from intermolecular interactions between the pyrene at the end of one molecule with pyrene at the end of a neighboring molecule, in the "open" lipid-bound conformation of the protein. To confirm such intermolecular interactions, cross-linking experiments employing N40C/L90C-apoLp-III were performed using the sulfhydryl-specific cross-linker bis-maleimidohexane (data not shown). Cross-linking of up to five molecules of apoLp-III per disk particle was observed, suggesting that the sulfhydryl groups are located at either end of an open molecule of apoLp-III in the lipid-bound configuration.

Relative Orientation of ApoLp-III Molecules on Discoidal Complexes. The presence of intermolecular pyrene−pyrene interactions in apoLp-III/phospholipid complexes prompted us to address questions related to the relative orientation apoLp-III adopts in discoidal complexes. In this case, pyrene-labeled N40C- or pyrene-labeled L90C-apoLp-III was complexed to DMPC vesicles to form a uniform population of discoidal bilayer complexes (*6*). In both cases, upon excitation at 345 nm, there was an absence of excimer fluorescence in the region around 460 nm (Figure 7, curves a and b). If the end of the apoLp-III molecule harboring the N40C residue is assigned as the "head" and that bearing L90C as the "tail", then a tandem arrangement of apoLp-III molecules may be envisioned. A precise "head-to-tail" orientation of apoLp-III, wherein N40C in one molecule is proximal to L90C from another, emerges from these studies. To further examine this ordered arrangement, disk complexes were prepared from equal amounts of pyrene-labeled N40C- and pyrene-labeled L90C-apoLp-III. In this case, excimer formation was observed, although it was not as intense as may be expected (Figure 7, curve c). It is conceivable that, although equal amounts of both single pyrene-labeled mutants were used to form the discoidal complexes, (i) equal amounts of pyrene-labeled mutants may not have been recovered in association with the disks or (ii) a random distribution of the labeled proteins on the disks may not have occurred.

DISCUSSION

Pyrene excimer fluorescence provides a useful tool to study apolipoprotein conformational changes which occur upon lipid interaction and to understand helix organization in the lipid-bound state of exchangeable apolipoproteins. This technique has been successfully used to obtain information about conformational alterations in other proteins including tropomyosin (*13*, *19*, *20*), troponin C (*21*, *22*), lactose permease (*23*, *24*), and sarcoplasmic reticulum ATPase (*25*). In the present study, *N*-(1-pyrene)maleimide was the extrinsic fluorophore of choice to study lipid binding-induced conformational changes in a model helix bundle apolipoprotein, permitting deduction of its relative orientation in discoidal complexes with phosphatidylcholine. Pyrene fluorophores serve as unique probes for the following reasons: (i) they possess a high extinction coefficient and the monomer has a long lifetime (up to 90 ns) (*26*); (ii) the maleimide derivative can be used to selectively label cysteine residues at specified sites on a protein; and (iii) excited pyrene monomers can interact with a neighboring ground-state pyrene, proximal in space, forming dimeric "excimer" complexes. The structure of pyrene crystals indicates that the pyrenes interact as dimers, stacked in a precise manner with a distance of 3.5 Å between the two planes (*27*). Comparison of the excitation and emission spectra of single-labeled N40C- or L90C-apoLp-III and double-labeled N40C/L90C-apoLp-III clearly shows the exception of excimers to the mirror-image rule (Figure 2) (*12*). The emission spectrum of single-labeled apoLp-III is a mirror image of its excitation spectrum as a result of the same transition being involved in both absorption and emission and the similarities among the vibrational energy levels of the ground and first-excited states. However, the emission spectrum of double-labeled apoLp-III is not a mirror image of its excitation spectrum, as the excimer emission is a result of an excited-state reaction which originates from a lower energy excited state than the excited monomer and dissociates upon returning to the ground state. Intrinsic excimer formation in apoLp-III arising from proximal aromatic residues [e.g., Tyr 145 and Phe 148; (*28*)] in the absence of pyrene labeling can be eliminated since selective excitation at 280 nm does not reveal emission at wavelengths longer than 306 nm for tyrosine residues (*M. sexta* apoLp-III lacks tryptophan residues) (*29*).

Pyrene-labeled N40C/L90C-apoLp-III displays a resistance to denaturation that is not observed for unlabeled apoLp-III (*10*). This may arise from stacking of the pyrene rings or, alternatively, pyrene interactions with aromatic residues present in the protein. It is recognized that aromatic interactions contribute to hydrophobic packing in proteins, especially when a network of Tyr, Phe, and Trp is present (*30*, *31*). While excimer emission arises only from stacked pyrenes, every stacked configuration does not lead to excimer emission. It appears that a range of stacked configurations is present in pyrene-labeled N40C/L90C-apoLp-III, as suggested by a simple numerical addition of the monomer emission spectra of the two pyrene-labeled single mutants (see Figure 2). Whereas monomer emission in the double-labeled protein is superimposable on that of the added

spectra, it should be less considering that a significant excimer peak appears. Thus, we conclude that different populations of monomer exist in the ground state, with a major portion forming excimers, and a smaller portion forming either unstacked pyrenes or stacked pyrenes which result in "dark complex" formation wherein the aromatic rings do not attain a precise excimeric configuration.

Pyrene Rings Proximal in the Lipid-Free Helix Bundle State. Pyrene excimer fluorescence occurs only when neighboring pyrenes reside ≤10 Å from one another (*14*). The occurrence of an excimer peak in double-labeled apoLp-III indicates proximity of the pyrene moieties attached to N40C and L90C in the helix bundle state. This interpretation concurs with the earlier observation that these two engineered cysteine residues are able to form a disulfide bond with each other (*5*) and confirmed by the NMR-derived solution global fold of apoLp-III, which reveals that the distance between N40 and L90 is about 9 Å (*3*). The possibility that intermolecular excimer formation occurs in this system can be eliminated since no change in the ratio of monomer to excimer emission was observed when lipid-free pyrene-labeled N40C/L90C-apoLp-III was diluted 8-fold. Furthermore, neither of the single-cysteine mutants displayed excimer fluorescence when labeled with pyrene.

Unfolding of Pyrene-Labeled ApoLp-III. Having demonstrated that the pyrene molecules are proximal in the lipid-free state of apoLp-III, we sought to determine whether changes in apoLp-III conformation could be manifest by changes in excimer quantum yield. Excimer fluorescence can be lost in three ways: (i) the protein undergoes a conformational change which distances the excited-state monomer from the second ground-state pyrene; (ii) the excited-state monomer may become quenched in aqueous solution, thereby preventing its interaction with a ground-state pyrene to form the excimer configuration; or (iii) the pyrenes are not stacked in the favorable configuration required to produce excimer fluroescence. Denaturation studies were carried out to validate the use of excimer fluorescence to study helix reorientation in apoLp-III. Our rationale was based on the fact that, under denaturing conditions, apoLp-III will unfold, forcing the pyrene-labeled helical segments in question to move away from one another. We hypothesized that such movement would be reflected by a decrease in excimer fluorescence and a corresponding increase in monomer fluorescence. When GdnHCl was used to denature pyrene-labeled N40C/L90C-apoLp-III, however, we noted a concentration-dependent loss in both monomer and excimer fluorescence. The decrease in pyrene monomer fluorescence is accounted for by increased exposure to bulk solvent (or GdnHCl), as seen by loss of monomer fluorescence in single pyrene-labeled N40C-apoLp-III as a function of GdnHCl concentration (data not shown). Since CD data show complete unfolding of the protein in high GdnHCl, the presence of residual excimer fluorescence is likely due to intermolecular interactions with neighboring unfolded proteins.

When pyrene-labeled N40C/L90C-apoLp-III was subjected to thermal denaturation, excimer fluorescence was lost. However, loss of excimer fluorescence coincided with a loss in monomer fluorescence which is attributed to thermally activated solvent quenching (*32, 33*). On the basis of this phenomenon, it is difficult to correlate the loss of excimer fluorescence directly to protein unfolding. In addition to its ability to disrupt tertiary and quarternary structure, previous studies have shown that TFE has a preferential interaction with hydrophobic domains in proteins (*34, 35*). Analogous to the manner in which helix−helix interactions are replaced by helix−lipid interactions upon lipid binding of helix-bundle apolipoproteins, we postulated that tertiary contacts in apoLp-III would be disrupted by TFE with helix−helix interactions in the bundle conformation replaced by helix−TFE interactions. If TFE disrupts helix−helix interactions in double pyrene-labeled apoLp-III, then we expect changes in excimer fluorescence. Increasing amounts of TFE resulted in an initial increase in the area under the excimer peak for pyrene-labeled N40C/L90C-apoLp-III. This may be explained by a tighter packing of the pyrene-labeled α-helical segments, an observation also noted in the case of the N-terminal domain of apolipoprotein E (*36*), another helix-bundle apolipoprotein. Subsequently, increasing TFE concentrations resulted in a steady decrease in the area under the excimer peak. While this may be due to increased flexibility of the helix bundle and movement of helices away from one another, the loss in excimer fluorescence was paralleled by a loss in monomer fluorescence. Indeed, in a separate experiment, when single pyrene-labeled N40C-apoLp-III was titrated with TFE, quenching of monomer fluorescence occurred. Taken together, the data indicate that exposure of pyrene-labeled apoLp-III to GdnHCl, TFE, or heat results in a loss of excimer fluorescence. This effect is likely a reflection of both the conformational state of the protein and the apparent quenching of monomer fluorescence, due to exposure to the bulk solvent. Interestingly, comparison of excimer excitation spectra under native and denaturing conditions (GdnHCl or heat) revealed that, although excimer fluorescence is lost, pyrene moieties retain stacked interactions.

Lipid-Induced Tertiary Structural Reorganization. When pyrene-labeled N40C/L90C-apoLp-III was complexed to discoidal particles, excimer emission was observed. Subsequently, experiments were performed to distinguish whether excimer fluorescence in disk-bound pyrene-labeled N40C/L90C-apoLp-III was due to intermolecular pyrene−pyrene interactions. We found that, unlike the lipid-free state, where dilution of the sample did not affect the ratio of monomer to excimer emission (suggesting intramolecular excimer formation), an increase in this ratio occurred when the proportion of pyrene-labeled double mutant apoLp-III was diluted with unlabeled wild-type apoLp-III on the surface of the disks (Figure 6). Hence, the decrease in the ratio of E/E_{100} emission is likely due to the fact that helices 2 and 3 reposition away from each other in the lipid-bound form. The low excimer fluorescence still present at the highest dilution (5% labeled apoLp-III) may be attributed to residual intermolecular pyrene interactions, although a small contribution from intramolecular pyrene interactions cannot be eliminated. The existence of intermolecular pyrene−pyrene interactions between neighboring apoLp-III molecules in DMPC discoidal complexes was further confirmed by cross-linking up to five apoLp-III molecules around the discoidal complex using a sulfhydryl-specific cross-linker. Most importantly, it should be noted that, while there is a significant change in excimer fluorescence, there is also an increase in the ratio of monomer fluorescence to excimer fluorescence as the amount of pyrene-labeled protein on the

disk complexes is decreased (corrected for dilution). Since the *m*/*e* ratio increases from 1.7 to 7.2 at the highest dilution, we attribute loss of excimer fluorescence to a decreased probability of forming intermolecular pyrene−pyrene interactions on the surface of the disk particles.

These results are consistent with previous studies that examined the conformation of apoLp-III in phospholipid disk complexes. Electron microscopic analysis reveals that DMPC/apoLp-III complexes are disk-shaped particles, 22 nm in diameter (*6*). Cross-linking experiments using dimethyl suberimidate (which cross-links lysine residues) indicate that up to six apoLp-III molecules align around the periphery of the disk complexes in an open state. Taken together, geometric calculations suggest that apoLp-III molecules orient with their helical axes perpendicular to the fatty acyl chains (*6*). This concept has been independently validated by attenuated total reflectance Fourier transform infrared spectroscopy studies (*37*). In this configuration, adjacent apoLp-III molecules on the same disk would be in close proximity.

Relative Orientation of Neighboring ApoLp-III Molecules in Disk Particles. Pyrene-labeled single-mutant apoLp-IIIs provided useful information regarding the orientation of the protein when bound to phospholipid disk particles. When either pyrene-labeled N40C-apoLp-III or pyrene-labeled L90C-apoLp-III was complexed to the phospholipid bilayer, no excimer fluorescence was observed. This observation suggests that the apoLp-III molecule binds to discoidal complexes in a nonrandom, ordered orientation. Such an ordered arrangement may arise from the fact that when the five-helix bundle opens, three helical segments in the bundle (helices 1, 2, and 5) move away from helices 3 and 4 as the molecule opens. If this helix arrangement is maintained, alignment of apoLp-III molecules in an ordered manner would create a three-helix/two-helix repeat around the disk perimeter (6). However, since the probes in the present study are localized to helices 2 and 3, the possible repositioning of helix 1 cannot be excluded without further studies. In the case of apoΔ(1−43)A-I, it has been shown that the protein aligns itself around the periphery of a disk, resembling a "belt structure" (*38*, *39*). Such an organization is also possible for the conformation of apoLp-III around discoidal complexes. Further studies, using different pyrene-labeled cysteine pairs, should yield additional insight into the binding of exchangeable apolipoproteins to lipid surfaces.

ACKNOWLEDGMENT

We thank Kim Oikawa and Robert Luty for assistance with GdnHCl/temperature denaturation and CD studies and Paul Semchuk for electro-spray mass spectrometric analyses.

REFERENCES

1. Fielding, C. J., and Fielding, P. E. (1995) *J. Lipid Res. 36*, 211−228.
2. Narayanaswami, V., and Ryan, R. O. (1997) *Biochem. Soc. Trans. 25*, 1113−1118.
3. Wang, J., Gagne, S., Sykes, B. D., and Ryan, R. O. (1997) *J. Biol. Chem. 272*, 17912−17920.
4. Breiter, D. R., Kanost, M. R., Benning, M. M., Wesenberg, G., Law, J. H., Wells, M. A., Rayment, I., and Holden, H. M. (1991) *Biochemistry 30*, 603−608.
5. Narayanaswami, V., Wang, J., Kay, C. M., Scraba, D. G., and Ryan, R. O. (1996) *J. Biol. Chem. 271*, 26855−26862.
6. Weintzek, M., Kay, C. M., Oikawa, K., and Ryan, R. O. (1994) *J. Biol. Chem. 269*, 4605−4612.
7. Wang, J., Narayanaswami, V., Sykes, B. D., and Ryan, R. O. (1998) *Protein Sci. 7*, 336−341.
8. Ryan, R. O., Schieve, D., Wientzek, M., Narayanaswami, V., Oikawa, K., Kay, C. M., and Agellon, L. B. (1995) *J. Lipid Res. 36*, 1066−1072.
9. Sahoo, D., Narayanaswami, V., Kay, C. M., and Ryan, R. O. (1998) *J. Biol. Chem. 273*, 1403−1408.
10. Ryan, R. O., Oikawa, K., and Kay, C. M. (1993) *J. Biol. Chem. 268*, 1525−1530.
11. Wu, C. W., Yarbrough, L. R., and Wu, F. Y. (1976) *Biochemistry 15*, 2863−2868.
12. Lakowicz, J. R. (1983) *Principles of Fluorescence Spectroscopy*, Plenum Press, New York.
13. Betcher-Lange, S. L., and Lehrer, S. S. (1978) *J. Biol. Chem. 253*, 3757−3760.
14. Lehrer, S. S. (1995) *Subcell. Biochem. 24*, 115−132.
15. Nelson, J. W., and Kallenbach, N. R. (1986) *Proteins: Struct., Funct., Genet. 1*, 211−217.
16. Sönnichsen, F. D., Van Eyk, J. E., Hodges, R. S., and Sykes, B. D. (1992) *Biochemistry 31*, 8790−8798.
17. MacPhee, C. E., Perugini, M. A., Sawyer, W. H., and Howlett, G. J. (1997) *FEBS Lett. 416*, 265−268.
18. Kiss, R. S., Kay, C. M., and Ryan, R. O. (1999) *Biochemistry 38*, 4327−4334.
19. Lin, T.-I. (1982) *Biophys. Chem. 15*, 277−288.
20. Burtnick, L. D., Sanders, C., and Smillie, L. B. (1988) *Arch. Biochem. Biophys. 266*, 622−627.
21. Liou, Y.-M., and Fuchs, F. (1992) *Biophys. J. 61*, 892.
22. Verin, A. D., and Gusev, N. B. (1988) *Biochim. Biophys. Acta 956*, 197−208.
23. Jung, K., Jung, H., Wu, J., Privé, G. G., and Kaback, H. R. (1993) *Biochemistry 32*, 12273−12278.
24. Jung, K., Jung, H., and Kaback, H. R. (1994) *Biochemistry 33*, 3980−3985.
25. Lüdi, H., and Hasselbach, W. (1983) *Eur. J. Biochem. 130*, 5−8.
26. Weltman, J. K., Szaro, R. P., Frackelton, R., Jr., Dowben, R. M., Bunting, J. R., and Cathou, R. E. (1973) *J. Biol. Chem. 248*, 3173−3177.
27. Birks, J. B. (1967) *Nature 214*, 1187−1190.
28. Lehrer, S. S., and Fasman, G. D. (1965) *J. Am. Chem. Soc. 87*, 4678.
29. Narayanaswami, V., Frolov, A., Schroeder, F., Oikawa, K., Kay, C. M., and Ryan, R. O. (1996) *Arch. Biochem. Biophys. 334*, 143−150.
30. Burley, S. K., and Petsko, G. A. (1985) *Science 229*, 23−28.
31. Newcomb, L. F., and Gellman, S. H. (1994) *J. Am. Chem. Soc. 116*, 4993−4994.
32. Birks, J. B. (1970) *Photophysics of Aromatic Molecules*, pp 301−370, Wiley-Interscience, New York.
33. Chandross, E. A., and Dempster, C. J. (1970) *J. Am. Chem. Soc. 92*, 3586−3593.
34. Lau, S. Y. M., Taneja, A. K., and Hodges, R. S. (1984) *J. Chromatogr. 317*, 129−140.
35. Rothemund, S., Weibhoff, H., Beyermann, M., Krause, E., Bienert, M., Mügge, C., Sykes, B. D., and Sönnichsen, F. D. (1996) *J. Biomol. NMR 8*, 93−97.
36. Fisher, C. A., and Ryan, R. O. (1999) *J. Lipid Res. 40*, 93−99.
37. Raussens, V., Narayanaswami, V., Goormaghtigh, E., Ryan, R. O., and Ruysschaert, J.-M. (1995) *J. Biol. Chem. 270*, 12542−12547.
38. Borhani, D. W., Rogers, D. P., Engler, J. A., and Brouillette, C. G. (1997) *Proc. Natl. Acad. Sci. U.S.A. 94*, 12291−12296.
39. Segrest, J. P., Jones, M. K., Klon, A. E., Sheldahl, C. J., Hellinger, M., De Loof, H., and Harvey, S. C. (1999) *J. Biol. Chem. 274*, 31755−31758.

BI992609M